

# Consequences of Magnocellular Dysfunction on Processing Attended Information in Schizophrenia

Antígona Martínez<sup>1,2</sup>, Steven A. Hillyard<sup>2</sup>, Stephan Bickel<sup>1</sup>, Elisa C. Dias<sup>1</sup>, Pamela D. Butler<sup>1,3</sup> and Daniel C. Javitt<sup>1,3</sup>

<sup>1</sup>Nathan Kline Institute for Psychiatric Research, Schizophrenia Research Division Orangeburg, NY 10962, USA, <sup>2</sup>Department of Neurosciences, University of California, San Diego, CA 92093, USA and <sup>3</sup>Department of Psychiatry, New York University Langone School of Medicine, New York, NY 10016, USA

Address correspondence to Antígona Martínez, Nathan Kline Institute for Psychiatric Research, 140 Old Orangeburg Road, Orangeburg, NY 10962, USA. Email: martinez@nki.rfmh.org.

**Schizophrenia is associated with perceptual and cognitive dysfunction including impairments in visual attention. These impairments may be related to deficits in early stages of sensory/perceptual processing, particularly within the magnocellular/dorsal visual pathway. In the present study, subjects viewed high and low spatial frequency (SF) gratings designed to test functioning of the parvocellular/magnocellular pathways, respectively. Schizophrenia patients and healthy controls attended to either the low SF (magnocellularly biased) or high SF (parvocellularly biased) gratings. Functional magnetic resonance imaging (fMRI) and recordings of event-related potentials (ERPs) were carried out during task performance. Patients were impaired at detecting low-frequency targets. ERP amplitudes to low-frequency gratings were diminished, both for the early sensory-evoked components and for the attend minus unattend difference component (the selection negativity), which is regarded as a neural index of feature-selective attention. Similarly, fMRI revealed that activity in extrastriate visual cortex was reduced in patients during attention to low, but not high, SF. In contrast, activity in frontal and parietal areas, previously implicated in the control of attention, did not differ between patients and controls. These findings suggest that impaired sensory processing of magnocellularly biased stimuli lead to impairments in the effective processing of attended stimuli, even when the attention control systems themselves are intact.**

**Keywords:** attention, ERP, fMRI, magnocellular, schizophrenia

## Introduction

Schizophrenia (SZ) is a complex mental illness associated with severe neurocognitive dysfunction, including impairments in attention. In the visual domain, attention deficits have been demonstrated using a variety of paradigms (reviewed in Luck and Gold 2008). The precise nature and underlying physiological bases of these deficits, however, remain poorly understood. One hypothesis is that attentional deficits in SZ reflect impaired executive allocation of attention (“control of selection”) while other aspects of attention, such as the implementation of selection, are intact (Wang and Fan 2007; Luck and Gold 2008). In recent years, deficits in early visual processing have been increasingly documented in schizophrenia (Butler et al. 2005, 2007; Martinez et al. 2008), and it has been suggested that these sensory processing deficits may play a role in impaired functioning of higher order cognitive mechanisms.

In primates, the primary visual pathway from retina to cortex includes anatomically and functionally distinct classes of neurons (Livingstone and Hubel 1987). Magnocellular neurons

respond preferentially (though not exclusively) to achromatic, moving stimuli of low contrast and low spatial frequency (SF), and project preferentially to the dorsal stream of visual cortical areas. In contrast, cells in the parvocellular pathway respond best to static high contrast stimuli having high SF and/or chromatic properties and project preferentially to ventral visual stream areas (Tootell et al. 1988).

The sensory processing deficits reported in SZ patients have primarily involved the magnocellular visual pathway, as manifest in behavioral (Butler et al. 2005), electrophysiological (Butler et al. 2007), and functional magnetic resonance imaging (fMRI) (Martinez et al. 2008) studies. Deficits have also been observed, however, in processing of stimuli that engage the parvocellular pathways (Slaghuis 1998) and in processes relying on ventral stream function, including object identification (Saccuzzo and Braff 1986; Slaghuis and Bakker 1995; Butler et al. 1996).

There is mounting evidence that sensory processing deficits may impact higher order perceptual functions including object and face recognition, grouping, perceptual closure, and reading (Doniger et al. 2002; Leitman et al. 2005; Kim et al. 2006; Revheim et al. 2006; Kurylo et al. 2007; Dias et al. 2011). The present study investigated the effects of impaired visual sensory function on the selective processing of attended versus unattended stimuli differing in SF content. SZ patients and age-matched controls selectively attended to sinusoidal gratings of low (magnocellularly biased) or high (parvocellularly biased) SF presented in a randomized sequence. High-density recordings of event-related potentials (ERPs) were obtained to evaluate the timing and selectivity of feature-guided attention to these stimuli, as well as evoked cortical activity reflecting low-level sensory processing of high and low SFs.

fMRI was carried out using the same stimuli and task in a separate group of subjects. Hemodynamic changes during epochs of sustained attention to high and low SF provided information regarding neural activity in visual cortical areas where selective attention exerts a modulatory influence on stimulus processing and in frontal and parietal areas which have been implicated in the control and allocation of attention (Corbetta 1998; Hopfinger et al. 2000; Corbetta et al. 2002; Astafiev et al. 2003; Liu et al. 2003).

Based upon our prior studies (Butler et al. 2007; Martinez et al. 2008; Sehatpour et al. 2010; Dias et al. 2011), we hypothesized that both the initial sensory analysis and the subsequent selective processing of attended low SF stimuli would be abnormal in SZ patients but that these processes would be relatively preserved for high SF stimuli. Such an outcome would reinforce the hypothesis that impaired sensory processing of magnocellular-biased stimuli in SZ may lead to

downstream deficits in the operation of multiple sensory-dependent processes, including attention, even when the top-down control mechanisms are intact (Javitt 2009b; Kantrowitz et al. 2009; Dias et al. 2011).

Materials and Methods

Subjects

Participants were 35 patients (33 males, mean age 38.8 ± 8.4 years) meeting DSM-IV criteria for schizophrenia assessed by Structured Clinical Interview for DSM-IV (SCID) (First et al. 1997) and 29 healthy volunteers (26 males, mean age 42.7 ± 6.1 years). Twenty-one of these patients (19 males) and 15 control subjects (all males) took part in the ERP experiment. The remaining 14 patients (14 males) and 14 controls participated in the fMRI study. Schizophrenia patients were recruited from outpatient and chronic inpatient clinics in the New York City area.

All patients were on a stable dose of antipsychotics at the time of testing. Healthy volunteers with a history of SCID-defined axis I psychiatric disorder were excluded. Patients and control volunteers were excluded if they had any neurological or ophthalmologic disorders that might affect performance or if they met criteria for alcohol or substance dependence within the last 6 months or alcohol/substance abuse within the last month. All participants had at least 20/32 (0.63) corrected visual acuity or better on the Logarithmic Visual Acuity Chart (Precision Vision).

Subject groups did not differ in age, Edinburgh score for handedness, gender, or ethnicity. As expected, compared with controls, SZ patients had reduced years of education ( $t_{62} = -5.44, P < 0.001$ ), Quick IQ scores (Ammons and Ammons 1962) ( $t_{62} = -4.31, P < 0.001$ ), and Hollingshead socioeconomic status (SES) scores ( $t_{62} = -10.14, P < 0.0001$ ). However, parental SES did not differ between the groups ( $t_{62} = 0.102, P > 0.9$ ), suggesting similar premorbid potential (Table 1).

Informed consent was obtained from all subjects after full explanation of procedures. Subjects were excluded if they had any neurological or ophthalmological disorders that might affect performance or if they met criteria for alcohol or substance dependence within the previous 6 months or alcohol/substance abuse within the previous month. Healthy volunteers with a history of SCID-defined Axis I psychiatric disorder were excluded.

Stimuli and Task

Stimuli were circular gratings sinusoidally modulated with a 2D Gaussian envelope and composed of a fundamental frequency of either 0.8 cycles per degree (cpd, low-frequency standards) or 5 cpd (high-frequency standards) (Fig. 1). These particular SFs were chosen based on findings from our previous studies (Martinez et al. 2001, 2008) showing that these 2 frequencies elicit distinct patterns of ERPs and

fMRI responses and that healthy subjects are able to selectively focus attention on the 2 standard frequencies used here. All stimuli subtended 6.5° of visual angle from the center to the outer edge and were delivered against a gray field that was isoluminant with the mean luminance of the gratings, which had a light/dark contrast of 70%.

Target stimuli consisted of infrequent ( $P = 0.2$ ) gratings having a slightly higher (6 cpd, high-frequency targets) or slightly lower (0.5 cpd, low-frequency targets) SF than their respective standards. Standard and target stimuli were presented one at a time in random order at the center of gaze for 100-ms duration and stimulus onset asynchronies (SOAs) varying randomly between 700 and 1100 ms. Subjects were instructed to maintain eye fixation on a central point which was visible on the screen at all times.

Two attention conditions (attend-high SF and attend-low SF) were administered in separate blocks of trials. At the start of each block subjects were instructed as to which SF was task relevant (high or low). The subject's task was to respond with a button press to the target gratings, which deviated slightly from the attended standard frequency. During ERP recordings, each attention block lasted 32 s. A single ERP run consisted of 6 blocks (3 attend-high and 3 attend-low blocks, in random order) and three 20-s rest blocks (fixation only) which were interspersed evenly during the run. Subjects took part in 12 runs. During fMRI scanning, the task was identical except that the rest condition lasted only 12 s and one run consisted of 8 attention blocks (4 attend-high, 4 attend-low). In the fMRI experiment, subjects took part in 2 such runs. Six blocks of practice trials (3 attend-high SF and 3 attend-low SF) were given to all subjects prior to ERP recordings and fMRI. Subjects undergoing fMRI additionally received one block of practice trials for each attention condition upon entering the magnet.

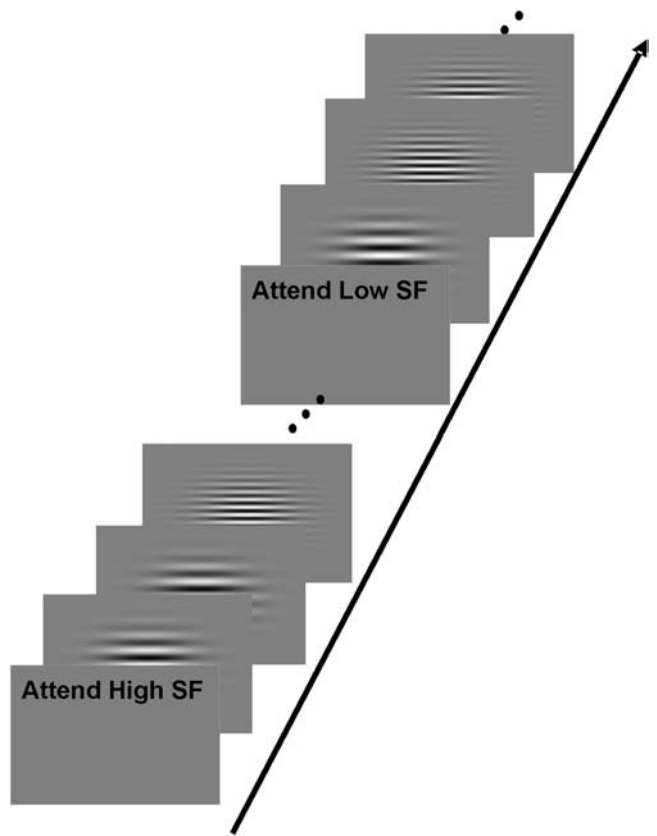


**Figure 1.** Experimental design. During separate blocks of trials, subjects were instructed to pay attention to either the high or low SF gratings and press a button upon detection of infrequent targets of the attended SF. Targets were of slightly higher (high SF targets) or slightly lower (low SF targets) SF than the relevant standard stimulus. High and low SF stimuli were delivered randomly and at a rapid rate in order to maintain a state of highly focused selective attention.

**Table 1**  
Sample characteristics for SZ patient and control participants

	Patients (n = 35)	Controls (n = 29)
Age	36.8	40
IQ (Quick IQ)**	96.1 (7.1)	106.3 (14.0)
Gender		
Male	33	26
Female	2	3
Years of education**	12.1 (1.5)	14.5 (2.2)
Participant SES**	25.1 (6.3)	45.3 (9.5)
Parental SES	40.6 (7.9)	44.5 (12.9)
CPZ equivalents (mg)	1201 (863.5)	—
Antipsychotics		
Typical	13	—
Atypical	17	—
Combination	5	—

Note: Standard deviations are indicated in parentheses.  
\*\* $P < 0.001$ .

Correct detection rates (hits) and mean reaction times (RTs) to targets and false alarms (FAs) to standards were recorded for each subject during the ERP experiment. Detection responses made within a window of 200–1200 ms following targets/standards were considered hits/FAs, respectively. Separate repeated measures analyses of variance (ANOVAs) were performed for each of these behavioral measures with a within-subject factor of SF (high or low) and a between-subject factor of Group (SZ, control). Due to limitations inherent in the block design used and the substantially lower number of targets presented, hit rates in the fMRI experiment are reported, but statistical analyses of behavioral data are restricted to that obtained during ERP recordings.

### Electrophysiological Recordings and Data Analysis

ERPs were recorded from 168 electrode sites using the BioSemi ActiveTwo system (BioSemi B.V., Amsterdam, Netherlands) using recording procedures previously described (Butler et al. 2007). Data were acquired at a sampling rate of 512 Hz and filtered offline using cutoffs of 0.1 and 100 Hz. ERPs from each electrode site were averaged separately for standard and target stimuli of each SF under each attention condition. These averages were digitally low-pass filtered with a Gaussian finite impulse function (3 dB attenuation at 46 Hz) to remove high-frequency noise produced by muscle activity and external electrical sources and then were digitally rereferenced to the average of the left and right mastoids. Epochs with amplitudes exceeding  $\pm 60 \mu\text{V}$  at any electrode were excluded from averaging. Additionally, ERPs elicited by standard stimuli that were preceded by a target stimulus within 1000 ms were removed from the average. On average, 22% of the trials for patients and 14% of the control subjects' trials were rejected.

As in previous studies, mean amplitude measures for the major sensory-evoked ERP components C1, P1, and N1 were taken within specified time windows encompassing the peak of each component (C1: 80–100 ms; P1: 120–140 ms; and N1: 170–190 ms poststimulus onset). Based on initial pilot studies, 20 ms latency windows ( $\pm 10$  ms on either side of the peak) were determined to encompass the period of maximal amplitude for each component of interest. In all cases, a single measurement of mean amplitude was taken across each latency interval. For each component, the chosen latency windows are in accord with those used in previous studies of attention to SF utilizing similar stimuli (Zani and Proverbio 1995; Martinez et al. 2001; Baas et al. 2002). For each component, the mean amplitude was calculated across 18 posterior electrode sites (9 per hemisphere, LH: E30–E32, A10–A15, RH: B7–B12) or 6 posterior midline sites (A19–A25), where the components of interest were maximal. Separate ANOVAs were performed for each component and for high and low SF separately, with within-group factors of attention (attended, unattended) and hemisphere (where appropriate left, LH; right, RH) and a between-group factor of group (SZ, control).

The effects of attention were manifested in the attentional difference wave formed by subtracting the ERPs elicited by unattended standard stimuli of each SF from ERPs elicited by the same stimuli when attended. From these difference waves, the timing (onset and duration) of the SF-related attention effects was determined by calculating pointwise ("running") *t*-tests of the amplitude of the difference potential relative to the mean amplitude of the prestimulus baseline. For each electrode, the first time point where the *t*-test exceeded the  $P < 0.05$  criterion for at least 10 consecutive data points (i.e., for  $> 20$  ms) was taken as the onset latency of the attention effect. The duration of the attention effect was taken as the time from the calculated onset point to the point at which 10 consecutive data points did not reach a  $P < 0.05$  criterion. As an additional measure of onset time for the attention effects, the half-amplitude latency (the time point at which the difference wave achieved 50% of its maximum amplitude within a specified time window) was calculated individually for the high and low SF attentional difference waves in the interval spanning from stimulus onset (0 ms) to 500 ms. These latency values were entered into an ANOVA and tested for significant differences between patient and control groups (Hansen and Hillyard 1980; Kiesel et al. 2008).

Finally, between-group attention effects on the amplitude of the attentional difference wave were tested by ANOVA in the latency intervals 200–260 and 260–320 ms poststimulus onset, corresponding to the early and late phases of the selection negativity (SN) component described in previous ERP studies of attention to nonspatial features

including SF (Zani and Proverbio 1995; Martinez et al. 2001; Baas et al. 2002) and color (Anllo-Vento et al. 1998). For each latency window, separate ANOVAs that included the factors group (SZ, control), SF (high, low), and hemisphere (left, right) were performed using the mean amplitude of the difference wave calculated across 18 posterior electrode sites (9 per hemisphere). In all cases, the amplitude was calculated with respect to the mean voltage over the 100 ms baseline preceding stimulus onset.

Target-related ERPs were analyzed by comparing the mean amplitude elicited by attended targets of each SF with the mean amplitude elicited by attended standard (nontarget) stimuli of the same SF. Only correctly detected targets were included in subsequent analyses. Repeated measures ANOVAs with factors of group, SF, hemisphere (for N2b analysis only) and stimulus (targets, nontargets) were carried out in 2 latency intervals, 280–360 and 500–650 ms, corresponding to the peaks of the N2b and P3 components, respectively, as in previous studies (e.g., Anllo-Vento et al. 1998). The N2b component was tested across the same left and right hemisphere clusters of posterior electrode sites used in previous analyses. Statistical tests of P3 amplitude were carried out using the mean voltage calculated across a cluster of 16 occipitoparietal electrode sites (E2, E1, A1, B1, C3, E22, E23, A2, B25, B26, E24, E25, A3, B2, B24, and A4).

### Source Localization

To estimate the cortical generators of the attention-related ERP components, source analysis was carried out using a distributed linear inverse solution based on a Local Auto-Regressive Average (LAURA, Grave de Peralta Menendez et al. 2001). LAURA estimates 3D current density distributions using a realistic head model with a solution space of 4024 nodes equally distributed within the gray matter of the Montreal Neurological Institute's average template brain. It makes no a-priori assumptions regarding the number of sources or their locations and can deal with multiple simultaneously active sources (for a review see Michel et al. 2001). The procedure was implemented using the CARTOOL software by Denis Brunet (<http://brainmapping.unige.ch/Cartool.htm>). All source localization analyses of the SN component were carried out based on the grand-averaged attentional difference waves in the same time windows used for statistical testing (200–260 and 260–320 ms).

### fMRI Acquisition and Data Analysis

$T_2^*$ -weighted echo-planar images (EPIs) (repetition time/echo time/flip angle = 2 s/40 ms/90°; voxel size = 4 mm<sup>3</sup>; matrix size 64 × 64) were acquired on a 3-T Siemens 32-channel timTRIO, equipped with gradient echo-planar capabilities optimized for brain imaging. During each of 2 scans, 192 volumes were acquired on 32 contiguous slices in the coronal plane beginning at the occipital pole. The first 4 volumes were discarded prior to all analyses to allow for stabilization of the blood oxygen level-dependent (BOLD) signal. Visual stimuli were back-projected onto a screen located within the magnet bore and viewed via a mirror system. For anatomical localization of functional data, high-resolution (1 × 1 × 1 mm<sup>3</sup>) images of the entire brain were acquired from each subject using a standard magnetization prepared rapid gradient echo sequence.

The fMRI data were analyzed with the Analysis of Functional Neuro-images (AFNI) software package (Cox 1996). Prior to statistical testing, the EPI images from each scan were realigned to the first included volume, linearly detrended, and slice time corrected. Individual subject data were statistically analyzed using a general linear model (GLM). For each subject, the fMRI time series (concatenated across 2 scans) was fit with regressors representing the timing of the 2 attention conditions (attend-high and attend-low SF). Motion parameter estimates were also included in the GLM as covariates. The resulting regression coefficients for each attention condition were normalized and converted to percent BOLD signal change. Individual subject maps of percent signal change were then coregistered with each individuals' high-resolution anatomical images and projected into Talairach coordinate space (Talairach and Tournoux 1988) before being spatially smoothed with a Gaussian kernel of 6 mm full-width at half-maximum.

Individual signal change maps associated with attention to high and low SF were entered into separate repeated measures ANOVA with the between-subject factor Group (patients, controls). Statistically significant

within-group effects were calculated with one-tailed *t*-tests of the normalized attend-high SF and attend-low SF signal change maps. In all cases, significance threshold levels and minimum cluster sizes were established using a Monte Carlo simulation based on the program AlphaSim, incorporated in the AFNI software suite. These calculations took into account the Gaussian filtering performed on the data and utilized a mask to exclude voxels lying outside the brain, prior to clustering. In all, simulations were carried out on a 3D grid consisting of 20 902 voxels ( $4 \times 4 \times 4$  mm each). Data are reported only for voxels with corrected *P* values  $< 0.01$  (uncorrected per-voxel threshold was  $P < 0.001$ ) belonging to clusters of 8 or more first-nearest neighboring voxels ( $>512$  mm<sup>3</sup>).

In a secondary analysis, 4 regions of interest (ROIs) for each attention condition were defined based on the principal activation foci identified in the within-group analyses. These ROIs were situated bilaterally on the fusiform gyrus (FG), the precuneus (pCun), the inferior parietal lobe (IPL) and frontally on the middle frontal gyrus (MFG). In all cases, the ROIs were based on the coordinates of the center of mass of activation clusters in each cortical area, averaged across both groups of subjects and extending 12 mm from the center of mass in each plane. For each subject, the percent signal change was calculated within each ROI under each attention condition. These values were entered into separate ANOVAs with factors of Group (patients, controls) and SF (attend-low, attend-high SF) as well as into an omnibus ANOVA using ROI (pCun, FG, IPL, MFG) as an additional factor.

## Results

### Behavioral Performance

Behavioral data and results are summarized in Table 2. Overall, significant group differences were obtained for both hit rate and FA rate ( $P < 0.002$  for both), with patients showing lower hit rates and higher FA rates for both high and low SF targets. Mean RTs did not differ between SZ and control subjects for either high or low SF targets. The only measure that showed significant group  $\times$  SF interaction was hit rate. Follow up *t*-tests indicated that this interaction was due to a significant group difference in the hit rate to low ( $t_{34} = 4.17$ ,  $P < 0.002$ ) but not high ( $t_{34} = 0.77$ ,  $P < 0.45$ ) SF targets. Specifically, compared with control subjects, patients had significantly lower hit rates for low SF, but not high SF, targets.

### Event-Related Potentials

ERPs were analyzed separately for high and low SF standard stimuli and for attend-high and attend-low SF conditions. For each subject group, difference waveforms (attended minus unattended ERPs) were calculated separately for low and high SF standard stimuli. Finally, ERPs elicited by targets of each SF were compared with the responses elicited by attended nontarget (standard) stimuli.

**Table 2**  
Behavioral performance

		Mean		Group control versus SZ		SF high versus low		Group $\times$ SF	
		Control	Patient	$F_{1,34}$	<i>P</i>	$F_{1,34}$	<i>P</i>	$F_{1,34}$	<i>P</i>
Hits (%)	HSF	62.50	58.40	10.081	0.003	0.400	0.531	11.322	0.002
	LSF	68.60	44.70						
RT (ms)	HSF	522.0	525.8	0.476	0.500	1.345	0.254	0.886	0.353
	LSF	504.8	524.0						
FA (%)	HSF	2.83	8.82	11.720	0.002	2.170	0.150	0.030	0.865
	LSF	1.46	7.08						

Note: Mean percentage of correctly detected targets (hits %), RTs, and percentage of FA responses (FA %) are given for each subject group as a function of whether the attended stimulus was of high or low SF content. Main effects and significance levels for each of these behavioral measure tested by ANOVA are also given.

### High SF Standard ERPs

For both SZ and control subjects, the sensory-evoked ERP waveforms elicited by attended and unattended high SF standard stimuli began with a sharply focused occipital negativity, the C1 component, onsetting at approximately 60 ms following stimulus onset. The C1 amplitude was measured over the interval 80–100 ms. The C1 was followed by a bilateral positive-going deflection (the P1, tested in the interval 120–140 ms) peaking in amplitude over inferior occipital scalp sites. No significant main effects or interactions of group, attention, or hemisphere were observed for either the C1 or the P1 potentials. High SF stimuli also elicited an N1 component (170–190 ms), peaking bilaterally at roughly 180 ms over the ventrolateral scalp in the attended and unattended ERP waveforms of both subject groups. N1 amplitude was significantly reduced in SZ compared with control subjects, though all other main effects and interactions were non-significant (Table 3, top). Plots of ERP waveforms and voltage topography maps of the C1, P1, and N1 components are shown in Figures 2A and 3A, respectively.

### Low SF Standard ERPs

As in previous reports (e.g., Martinez et al. 2001), low SF stimuli did not elicit a C1 component. Rather, the first ERP component elicited by attended and unattended low SF standards was a bilateral P1 distributed over the dorsal occipital scalp at 80–100 ms and shifting to ventral occipital scalp sites in the interval 120–140 ms (Figs 2B and 3B and Table 3, bottom). Unlike for high SFs, a significant group difference in P1 amplitude to low SF stimuli was obtained in the 80 to 100 and 120 to 140-ms intervals, reflecting significantly diminished amplitudes in both the attended and the unattended waveforms of SZ subjects, compared with controls. Likewise, a main effect of group was obtained in the N1 latency window (170–190 ms) due to significantly reduced amplitudes in the patient waveforms. There were no significant main effects of attention or hemisphere on either the P1 or the N1 components, but the attention  $\times$  group interaction approached significance for the N1 due to its overlap with the initial phase of the SN (see below).

### Selective Attention Effects

The effects of selective attention to stimuli of high and low SF were analyzed in the difference waveforms formed by subtracting the ERPs elicited by attended standards from the ERPs elicited by the same stimuli when unattended (Fig. 4). These difference waves revealed a broad SN elicited preferentially by the attended stimuli, which was bilaterally distributed over ventrolateral occipital scalp sites. Running *t*-tests of the amplitude of the SN versus the prestimulus baseline were used to assess its onset and duration for high and low SF stimuli in each subject group (see Materials and Methods). In the case of attention to high SF, the onset of the SN was very similar for SZ and control subjects (217 and 209 ms, respectively, but the SN persisted longer in the patients than the controls (lasting until 375 vs. 325 ms). In contrast, the onset of the SN associated with selection of low SFs differed markedly between SZ and control subjects; whereas in controls, the SN began at 174 ms, in the patient waveforms, the onset of the SN was delayed by over 50 ms, beginning at 229 ms poststimulus onset. In both groups, however, the SN to the low SF stimuli persisted until about 360 ms. Similar effects were obtained when using the half-amplitude fractional latency as a measure of onset time for the

**Table 3**

ERP amplitudes elicited by high and low SF standard stimuli

		Control		SZ patients		Group		Attention		Group × Attention	
		Voltage/SEM (μV)				Control versus SZ		Attd. versus Unatt.			
Latency (ms)	Elec.	Attd.	Unatt.	Attd.	Unatt.	<i>F</i> <sub>1,33</sub>	<i>P</i>	<i>F</i> <sub>1,33</sub>	<i>P</i>	<i>F</i> <sub>1,33</sub>	<i>P</i>
High SF											
80–100	Mid.	−1.01/0.26	−1.09/0.38	−1.08/0.25	−1.17/0.11	0.049	0.831	0.205	0.653	0.010	0.993
120–140	LH	1.98/0.24	1.89/0.18	1.68/0.23	1.76/0.15	2.512	0.123	0.041	0.841	3.455	0.073
	RH	1.94/0.25	1.76/0.30	1.38/0.11	1.5/0.19						
170–190	LH	−0.45/0.20	−0.54/0.20	0.08/0.22	0.32/0.26	5.311	0.028	0.563	0.464	0.877	0.356
	RH	−0.71/0.20	−0.65/0.21	0.57/0.18	−0.01/0.26						
Low SF											
80–100	Mid.	0.72/0.13	0.73/0.13	0.26/0.06	0.19/0.05	15.342	0.001	1.171	0.287	2.381	0.132
120–140	LH	2.65/0.20	2.72/0.18	1.72/0.15	1.77/0.12	11.861	0.002	1.152	0.291	1.456	0.238
	RH	2.83/0.26	2.75/0.26	1.54/0.15	1.96/0.16						
170–190	LH	−1.29/0.18	−1.11/0.12	−0.18/0.16	−0.24/0.22	23.280	0.001	0.078	0.962	3.671	0.064
	RH	−1.38/0.19	−1.35/0.19	−0.40/0.10	−0.53/0.13						

Note: Mean voltage amplitudes along with standard error of the mean (SEM) (in microvolts) elicited by high SF (top) and low SF (bottom) standards when attended (Attd.) and unattended (Unatt.) are given separately for control subjects and SZ patients. Amplitudes were measured across clusters of electrodes in the left (LH) and right (RH) hemispheres and across midline (Mid.) scalp regions (Mid.). Values are given for 3 latency windows corresponding to the peaks of the short-latency sensory-evoked ERP components C1 (80–100 ms), P1 (120–140 ms), and N1 (170–190 ms).  $F$  values and significance ( $P$ ) levels resulting from ANOVA testing group differences (controls vs. patients), attention (attended vs. unattended), and the interaction of group and attention for high and low SF standards are given in 3 rightmost columns.

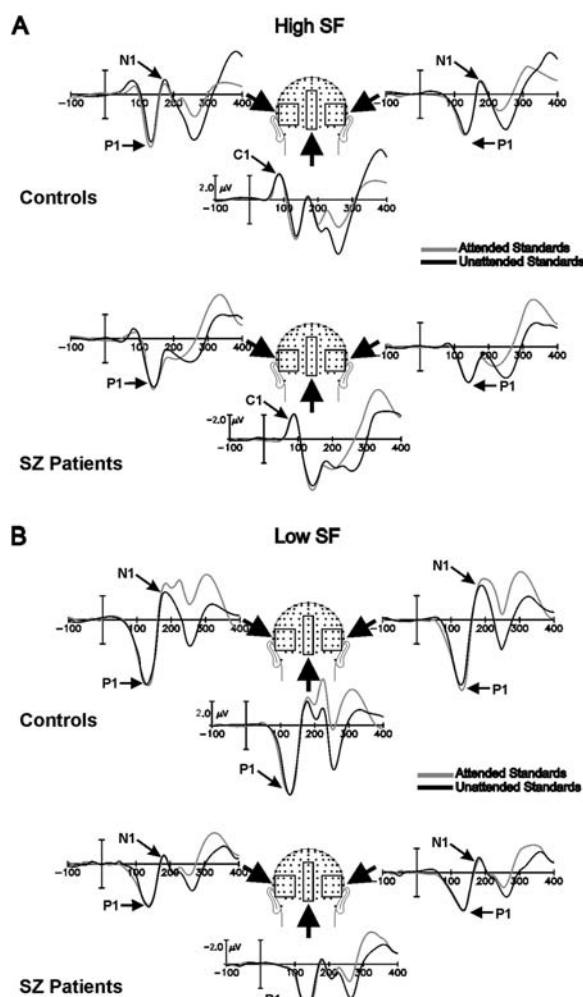


**Figure 2.** ERPs elicited by high and low SF standards. Grand-averaged ERPs elicited by high (A) and low (B) SF standards when attended (gray tracings) and unattended (black tracings) in control subjects and SZ patients. Data shown are mean voltage measured across 3 clusters of posterior electrode sites (depicted in outlined rectangles). ERP waveforms are plotted negative voltage up.

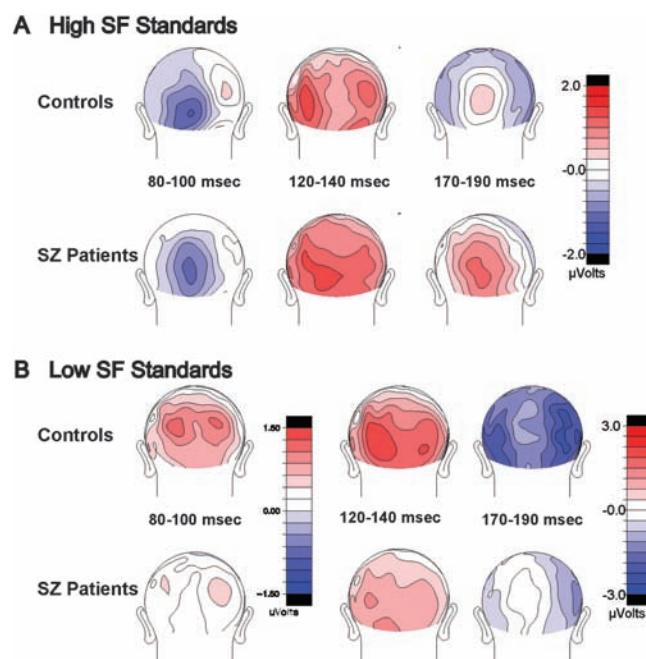


**Figure 3.** Voltage topography of unattended high and low SF standards. Mean voltage topography maps of latency windows corresponding to peaks of principal sensory-evoked components elicited by (A) high SF standards when unattended; C1 (80–100 ms), P1 (120–140 ms), and N1 (170–190 ms) and (B) unattended low SF standards; P1 in its early (80–100 ms) and late (120–140 ms) phases and N1 (170–190 ms). Data are shown for control subjects (top row of each group) and SZ patients (bottom row). For high SF maps, color scale on right applies to all maps. For low SF, maps of early P1 are on separate scale shown to the right.

high and low SF SNs; while there was no overall difference between groups, there was a highly significant interaction between group and SF ( $F_{1,34} = 36.77$ ,  $P < 0.0001$ ), reflecting the longer latency onset of the SN to low (but not high) SFs in SZ patients versus controls.

The mean amplitude of the SNs to high and low SF were tested by ANOVA within 2 latency intervals, 200–260 and 260–320 ms, encompassing early and late phases of the SN. The

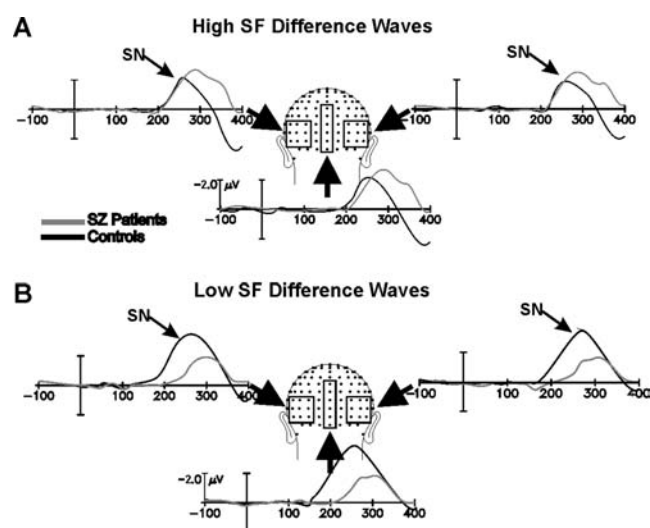
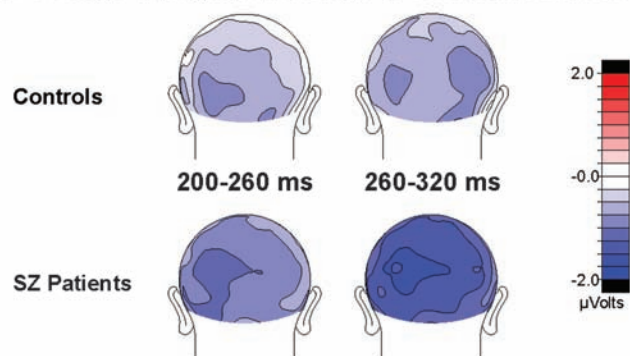


**Figure 4.** Effects of selective attention to high and low SFs. Attentional difference waves (attended minus unattended standards) highlighting the SN associated with attention to high (A) and low (B) SF stimuli are shown for 3 electrode clusters (depicted by outlined boxes). Gray tracings are grand-averaged ERPs from SZ patients. Black tracings are grand-averaged ERPs from control subjects. Negative voltage is plotted up.

#### A Voltage Topography of High SF Difference Waves



#### B Voltage Topography of Low SF Difference Waves

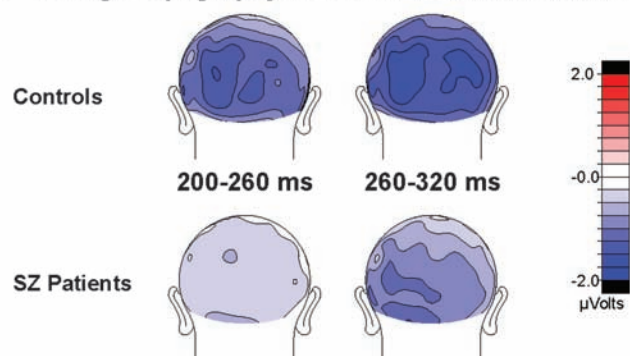


**Figure 5.** Topography of selective attention effects. Scalp voltage topography maps of high SF SN (A) and low SF SN (B). Mean SN voltage in 2 latency windows (200–260 ms and 260–320 ms) are shown for control subjects (top row of each group) and SZ patients (bottom row).

topographical distributions of SNs of the patients and controls in each interval are shown in Figure 5. Overall, the amplitude of the SN during the first time window (200–260 ms) was significantly

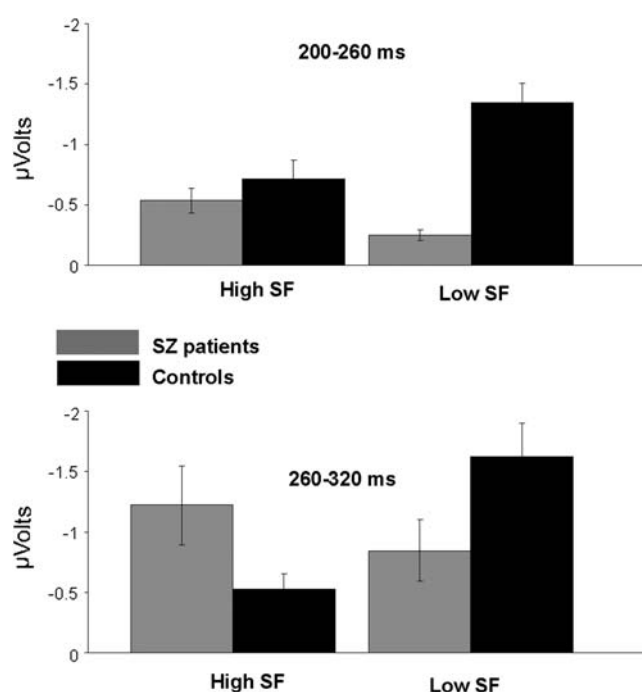


**Figure 6.** High and low SF SN amplitude. Mean amplitudes (averaged across both hemispheres) of the SNs associated with attention to high and low SF in the 2 intervals tested by ANOVA, 200–260 ms (top graph) and 260–320 ms (bottom graph). Values derived from grand-averaged SZ patient difference wave are shown in gray and from grand-averaged control subject waveform in black. Amplitude values of the SN to high SF are shown in striped-pattern bars, solid-pattern bars are for the SN to low SF. Error bars depict standard error of the mean.

larger (more negative) in control, relative to SZ, subjects ( $F_{1,34} = 49.02$ ,  $P < 0.0001$ ), and it was larger in the left, compared with right, hemisphere ( $F_{1,34} = 4.71$ ,  $P < 0.036$ ). Additionally, across both subject groups, the SN associated with low SFs was significantly larger than the SN to high SF stimuli ( $F_{1,34} = 4.14$ ,  $P < 0.050$ ). A significant group  $\times$  SF interaction ( $F_{1,34} = 29.31$ ,  $P < 0.001$ ) was obtained in the 200 to 260-ms interval, reflecting greater amplitudes of the SN to low SF stimuli in control subjects compared with patients ( $t_{34} = 8.32$ ,  $P < 0.001$ ) but there was no group difference in the magnitude of the SN to high SF stimuli ( $t_{34} = 1.52$ ,  $P < 0.137$ ) (Fig. 6, top). No other statistically significant effects or interactions were obtained in this interval.

In the second latency interval (260–320 ms), the SN to low SF stimuli was again marginally larger than to high SF stimuli overall ( $F_{1,34} = 4.14$ ,  $P < 0.050$ ). The interaction between SF and group was also highly significant ( $F_{1,34} = 17.29$ ,  $P < 0.001$ ) and was due to a significantly larger SN to high SF stimuli in patients ( $t_{34} = -2.03$ ,  $P < 0.049$ ) as well as a significantly larger SN to low SF stimuli in control subjects ( $t_{34} = 2.26$ ,  $P < 0.030$ ) (Fig. 6, bottom). No other effects in this interval were statistically significant.

A correlational analysis between the amplitude of the sensory-evoked P1 component (at 120–140 ms) for low SFs and the amplitude of the SN to low SF (at 260–320 ms) showed that, across groups, larger P1 amplitudes were associated with larger (more negative) SN amplitudes (Pearson's  $r = -0.37$ ,  $P < 0.01$ ). This effect was also significant when tested just within SZ patients (Pearson's  $r = -0.47$ ,  $P < 0.01$ ) though only in the LH where the SN was largest (in the RH, the effect was in the same direction and approached significance,  $r = -0.31$ ,  $P < 0.08$ ). In a further analysis, the amplitude of the SN to low SFs (averaged for LH and RH) was tested in a one-way between-group

ANOVA. As expected, this yielded a significant main effect of Group ( $F_{1,34} = 5.11$ ,  $P < 0.03$ ). When P1 amplitude (averaged for LH and RH) was added to the analysis as a covariate, the significant group difference was eliminated ( $F_{1,32} = 1.44$ ,  $P > 0.24$ ), providing further evidence of the correlation between the sensory-driven visual response reflected by the P1 and the subsequent attention-related SN.

### Source Localization Analyses

The LAURA algorithm was used to estimate the anatomical locations of the neural sources of the SNs to high and low SF stimuli in the intervals 200–260 and 260–320 ms. In both latency, windows LAURA identified a prominent ventral-occipital source associated with attention to high SF. This source was situated bilaterally in the FG (Brodmann's area, BA, 37; mean center of current density in Talairach coordinates =  $\pm 40$ ,  $-63$ ,  $-10$ ; Fig. 7) and was present in both subject groups.

Like attention to high frequencies, attention to low SF was associated with a ventral-lateral occipital source situated bilaterally (though stronger in the LH) in posterior regions of the FG (BA 19,  $\pm 33$ ,  $-74$ ,  $-12$ ) (Fig. 7). The strength of the SN source to low SF stimuli was markedly reduced, however, in SZ patients. In addition to the ventral source, LAURA identified a dorsal occipital source associated with attention to low SF in the superior occipital gyrus of the right hemisphere (not shown) (BA19;  $34$ ,  $-76$ ,  $26$ ). This source was only present in control subjects.

### Target-Elicited ERPs

ERPs elicited by high and low SF targets in the target minus standard difference waves (the difference wave formed by subtracting the ERPs elicited by nontarget stimuli from those elicited by target stimuli) are shown in Figure 8. An N2b component, elicited by relevant targets of both SFs, peaking in amplitude between 280 and 360 ms over ventral-occipital electrode sites, was significantly smaller overall for SZ versus control subjects ( $F_{1,34} = 16.68$ ,  $P < 0.001$ ). There were no other significant main effects or interactions in the N2b latency interval.

The P3 (also termed P3b) component peaked in the 500–650 ms range over centroparietal scalp regions. Overall, low SF

targets elicited significantly larger P3's than did high-frequency targets ( $F_{1,34} = 13.63$ ,  $P < 0.001$ ). As with the N2b, the P3 was significantly smaller across both SFs in SZ versus control subjects ( $F_{1,34} = 9.45$ ,  $P < 0.005$ ). Though only approaching statistical significance, this group difference in P3 amplitude was larger for low, compared with high, SF targets (Group  $\times$  SF:  $F_{1,34} = 3.83$ ,  $P < 0.06$ ).

### Functional Magnetic Resonance Imaging

Areas with significant responses during attention to high and low SF were evaluated separately within each subject group. In SZ patients and control subjects, attention to both high and low frequencies resulted in prominent activations in ventral-occipital cortex in the FG and the pCun of both hemispheres. Significant activations were also obtained in the IPL and in frontal cortex along the MFG (Table 4). Analysis of mean percent signal change within the ROIs defined by these regions (FG, pCun, IPL, and MFG) showed no significant main effects of Group or Hemisphere, nor significant Group  $\times$  Hemisphere interactions, during attention to high SF (all  $P > 0.30$ , Fig. 9A).

In contrast, significant group differences were obtained during attention to low SF in the FG and pCun, near the locations identified in the LAURA analyses as putative sources of the SN to low SF (Table 4). Within both these occipital regions, patients compared with controls, had significantly reduced activations resulting in a significant main effect of Group (FG:  $F_{1,26} = 16.57$ ,  $P < 0.0001$ ; pCun:  $F_{1,26} = 7.51$ ,  $P < 0.001$ ). In controls, the activation in the pCun region was larger in the RH, whereas in patients, pCun activations were larger in the LH leading to a significant Group  $\times$  Hemisphere interaction ( $F_{1,26} = 8.99$ ,  $P < 0.006$ ). As with attention to high SF, there were no significant group differences in the parietal or frontal ROIs during attention to low SF ( $P > 0.50$ , both). The only other significant effect associated with attention to low SF was a main effect of Hemisphere in the MFG, reflecting the generally larger activations in the right versus left hemisphere ( $F_{1,26} = 7.27$ ,  $P < 0.012$ ; Fig. 9B).

Finally, the comparison of attention to high versus low SF revealed significant Group  $\times$  SF effects in the pCun and FG ROIs (especially in the RH) but not in the ROIs for the IPL or MFG (Table 5 and Fig. 9C). Additionally, testing across all ROIs

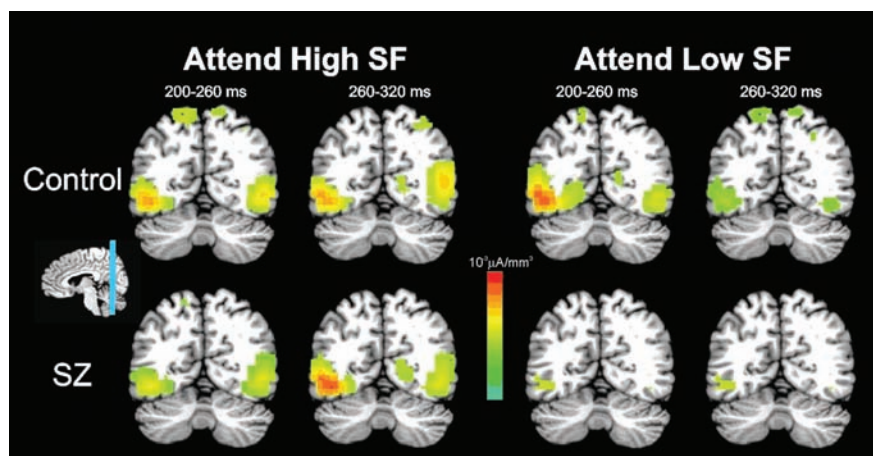


**Figure 7.** Anatomical sources of high and low SF SN. Estimated sources for the control subject and SZ patient grand-averaged SN (over 200–260 ms) associated with attention to high (A) and low (B) SF. The sources were modeled using the LAURA algorithm. Results are shown on a standardized brain in Talairach coordinates. The anterior–posterior position of the coronal slice shown is indicated on the sagittal slice on left. The LAURA inverse solutions are represented in red to green color scale indicating units of current source density ( $\mu\text{A}/\text{mm}^3$ ). In coronal sections, left hemisphere is on the left.

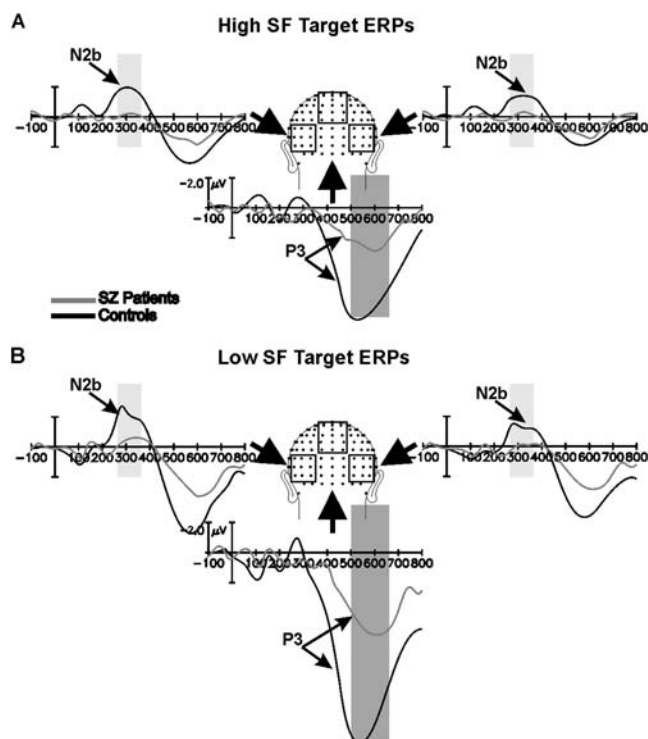


**Figure 8.** ERPs elicited by high and low SF targets. (A) ERPs elicited by high SF standards when attended were subtracted from the ERPs elicited by high SF targets. The resulting waveforms are shown for SZ patients (gray tracings) and control subjects (black tracings) for 3 clusters of electrodes (indicated by outlined boxes) where the N2b and P3 components were maximal. The shaded regions indicate the latency windows used for statistical testing of N2b (light gray, 280–350 ms) and P3 (dark gray, 500–650 ms) amplitudes. (B) Standard minus target difference waves, as described above, for low SF stimuli.

**Table 4**

Talairach coordinates and mean volume of cortical regions significantly activated during attention to high and low SF

	LH	RH
Attend High SF		
pCun (BA7)	–25, –61, 37 (2432/1728)	28, –65, 38 (1920/2176)
FG (BA19)	–42, –66, –11 (4288/4992)	41, –68, –13 (4992/4736)
IPL (BA40)	–41, –40, 33 (1280/1984)	43, –36, 36 (1664/1600)
MFG (BA9/46)	–40, 28, 20 (3200/3456)	35, 32, 29 (5184/4416)
Attend Low SF		
pCun (BA7)	–24, –63, 37 (1280/768)	22, –67, 38 (2944/512)
FG (BA19)	–37, –68, –11 (4736/896)	37, –67, –12 (6016/1600)
IPL (BA40)	–40, –41, 37 (1152/1472)	43, –42, 39 (2048/1792)
MFG (BA9/46)	41, 30, 23 (1856/3072)	37, 32, 20 (5312/5568)

Note: For SZ patients and control subjects, the average Talairach coordinates ( $x, y, z$ ) of cortical ROIs (corresponding BA in parentheses) with significant activations during attend-high (top) and attend-low (bottom) SF are provided for left (LH) and right (RH) hemispheres separately. The mean volume (in cubic millimeters) of each of these regions is given in parentheses for controls/patients.

revealed a highly significant 3-way interaction ( $\text{ROI} \times \text{Attention} \times \text{Group}$ ;  $F_{6,21} = 3.77$ ,  $P < 0.01$ ) reflecting the differential impairment in the patient group for low SFs, in posterior (FG, pCun) versus anterior (IPL, MFG) regions on this task.

## Discussion

Attentional deficits have long been considered a major feature of SZ. The present study used both ERP- and fMRI-based measures

to investigate the relationship between dysfunctional visual sensory analysis (Butler et al. 2005, 2007; Martinez et al. 2008) and the ability to selectively process attended visual information. In the ERP study, both sensory- and attention-related processing of parvocellularly biased stimuli was relatively intact in SZ patients. In contrast, patients showed deficient sensory processing of magnocellularly biased stimuli along with impaired processing of those stimuli when attended. Similarly, in the fMRI study, whereas there were no group differences in activations within frontal and parietal regions associated with the control and guidance of feature-selective attention, SZ patients showed significantly reduced activations in posterior regions belonging to sensory visual cortex, but only for attended magnocellularly biased stimuli. Together, these findings suggest that attentional deficits in SZ may result, at least in part, from impaired bottom-up sensory processing even when the top-down attentional control mechanisms are relatively intact.

In the present study, sinusoidal gratings of high and low SF were utilized to test functioning of the parvocellular and magnocellular pathways, respectively, by means of ERP recordings along with source localization and fMRI. Although SF manipulation does not fully dissociate the magno- and parvocellular visual systems, prior studies suggest that high and low SFs can effectively bias responses toward 1 of the 2 systems. For example, we have previously demonstrated differential anatomical patterns of fMRI activation to stimuli of varying SF in a manner consistent with different underlying pathways (Martinez et al. 2008). Similarly, ERP studies (e.g., Martinez et al. 2001; Schechter et al. 2005; Butler et al. 2007; Foxe et al. 2008) suggest differential contributions of the magnocellular and parvocellular pathways to specific sensory-evoked ERP components, consistent with the current finding of larger C1 potentials elicited by high versus low SF stimuli.

In the ERP study reported here, it was found that patients were selectively impaired at detecting targets of low SF and had generally diminished ERP amplitudes to stimuli of low SF, both for the early sensory-evoked components and for the negative difference component elicited by attended stimuli (the SN). Specifically, the deficit in early sensory analysis of low SFs resulted in diminished amplitude of the evoked P1 component which in turn was significantly correlated with impaired selective processing of attended stimuli as indexed by reduced amplitude of the SN component. In the parallel fMRI study, activations in extrastriate visual cortex were significantly reduced in SZ patients during attention to low SF but not during attention to high SF. In contrast, activations within frontal and parietal areas involved in the control and allocation of feature-guided attention did not differ between patients and controls, suggesting that the observed deficits in selective processing of low SFs observed in SZ patients were not a consequence of dysfunction in the top-down mechanisms that guide visual attention. We conclude that deficits in the early stages of sensory/perceptual encoding of visual information are a contributing factor to impairments in the selective processing of attended information in SZ, which result from the impoverished nature of the sensory information upon which attentional systems must operate. Importantly, once these deficits are taken into account, we find no additional evidence for attentional dysfunction within the feature attention system in SZ.

Several previous studies have shown that normal observers can selectively focus attention on one SF in preference to others, thereby facilitating the detection of targets that share the attended SF (Davis and Graham 1981; Miller 1981; Shulman

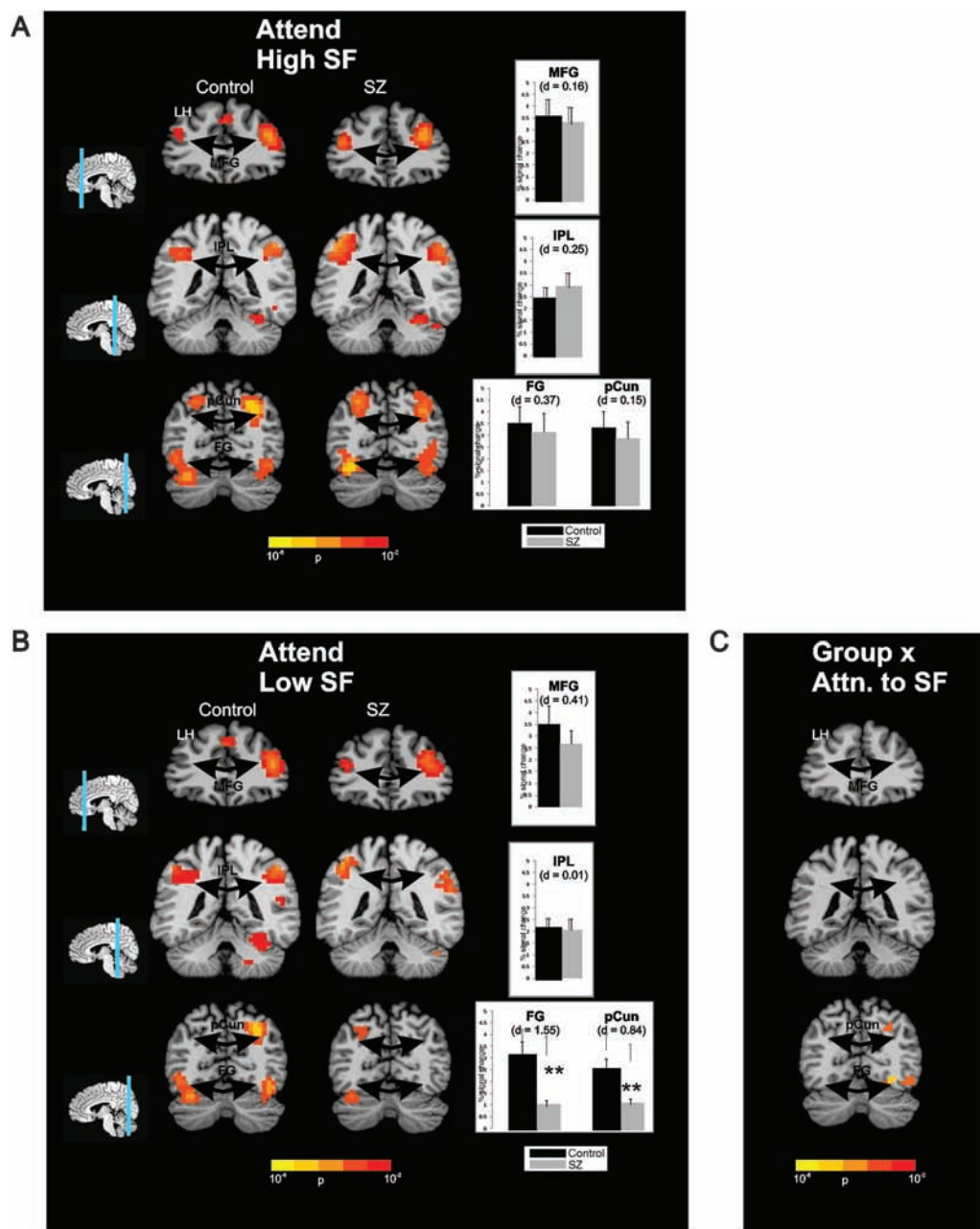


**Figure 9.** Cortical activations during attention to high SF. (A) For both SZ patients (right column) and control subjects (left column), attention to high SF resulted in bilateral activations in the FG and pCun (bottom row), the IPL (middle row), and frontally in the MFG (top row). For each cortical area, the mean percent signal change (averaged across left and right hemispheres) for controls (black bars) and patients (gray bars) is plotted to the right (arrow bars depict standard error of the mean). There were no significant group differences in any of these regions. (B) In frontal (MFG, top row) and parietal (IPL, middle row) cortical areas, selective attention to low SF produced very similar patterns of activation in patients (right column) and controls (left column). Activations within occipital regions, however, differed significantly with patients showing significantly reduced percent signal change in both the FG and the pCun. Mean percent signal change values are given on bar graphs to the right. For each region and attention condition, statistical effect size of the group difference is expressed in Cohen's *d* value and significance ( $P < 0.01$ ) is depicted with asterisks. (C) Regions with a significant Group (patients, controls)  $\times$  SF (attend-high, attend-low) interaction derived from maps shown in A and B. In all images, the left hemisphere is shown on left and color scale depicts corrected *P* values. The anterior-posterior location of each coronal slice shown is depicted on sagittal slice to the left.

et al. 1986; Shulman and Wilson 1987). This ability to selectively enhance the perception of stimuli at different spatial scales (e.g., the forest vs. the trees) is an important mechanism by which normal observers isolate relevant information from noisy visual environments (Davis and Graham 1981; Watson and Robson 1981; Graham et al. 1985). A robust electrophysiological manifestation of attention to SF is the broad SN elicited over the posterior scalp and superimposed on the sensory-evoked ERP components. The SN is proposed to

index neuronal activity within ventral extrastriate areas specialized for the processing of the attended feature dimension (Harter and Aine 1984; Hillyard and Anllo-Vento 1998). These enhanced neural responses in the visual cortex are generally considered to be modulatory effects under the control of efferent (top-down) projections from higher order brain regions involved in directing attention (Harter and Aine 1984; Anllo-Vento and Hillyard 1996; Heslenfeld et al. 1997; Anllo-Vento et al. 1998; Martinez et al. 2001; Baas et al. 2002).

**Table 5**

ROI analysis of fMRI activations during attention to high versus low SF in SZ patients versus control subjects

ROI	Group $F_{1,26}$	SF $F_{1,26}$	Group $\times$ SF $F_{1,26}$
pCun	6.64 (0.01)	1.31 (0.29)	4.93 (0.03)
FG	8.57 (0.007)	2.09 (0.16)	4.76 (0.02)
IPL	0.35 (0.56)	0.69 (0.42)	0.41 (0.53)
MFG	1.17 (0.29)	0.04 (0.85)	0.02 (0.89)

Note: ANOVA on mean percent signal change in each ROI revealed a significant Group (patients, controls)  $\times$  SF (attend-high, attend-low) interaction in the pCun and FG, reflecting significantly reduced activations in the patient group during attention to low, but not high, SF within these regions only.

In the present study, the SNs elicited during selection of high and low SF stimuli were differentially impaired in SZ patients compared with controls. Whereas the onset latency of the SN to low SF stimuli was significantly delayed in SZ patients, no group difference in onset latency was found for the SN to high SFs. Moreover, whereas the amplitude of the SN to low SF was significantly diminished in the SZ patients, the SN associated with attention to high SF was equivalent, or even larger, in patients compared with controls, and it persisted significantly longer in patients. One hypothesis to account for this persistence would be that patients have greater difficulty in disengaging attention from local or high SF stimulus features. This hypothesis follows from findings from a recent divided attention study utilizing hierarchical stimuli ("global" vs. "local" features) in which SZ patients showed significant interference effects of local on global processing, whereas control subjects showed the opposite pattern (Coleman et al. 2009).

Source localization analyses of the ERP selective attention effects to both high and low SFs confirmed prior reports of prominent neuroanatomical generators for the SN in ventral occipital regions of visual cortex (Hillyard and Anllo-Vento 1998; Martinez et al. 2001; Baas et al. 2002). The magnitudes of the intracranial sources associated with attention to low, but not high, SF were markedly reduced in SZ patients, consistent with the observed differential impairment in selection of low versus high SF stimuli. These source localizations obtained for the SN coincide well with the current fMRI findings of prominent clusters of activation in ventral occipital cortex during attention to high and low SF. This spatial coincidence provides evidence that the scalp-recorded SN and the parallel fMRI activations are derived from a common source of attention-related neural activity.

Significant impairments in the SZ group were also evident in the ERPs elicited by target stimuli. As in previous reports (e.g., Arnott and Alain 2002; Potts et al. 2002), the N2b component was significantly reduced in patients, suggesting a deficit in the discrimination and classification of both high and low SF targets. This N2b reduction was paralleled by an increased FA rate in the patients in response to both target types. The amplitude of the P3 (P300) component was also significantly reduced in SZ patients in agreement with many previous studies (e.g., Kemali et al. 1991; Ford et al. 1994; Potts et al. 2002; Wood et al. 2007). This reduction in P3 amplitude was seen for both high and low SF targets, but the low SF targets elicited a relatively smaller P3 than the high SF targets at a marginal level of significance. Behaviorally, these reduced P3 amplitudes were paralleled by differential group differences in target detection accuracy, with SZ patients being significantly less accurate than controls at detecting low, but not high, SF targets. Interestingly, the mean RTs to targets did not

significantly differ between groups, possibly due to the short SOAs used in this study, which may have forced patients to trade off accuracy for speed, thereby incrementing their FA rates.

The combined ERP, fMRI, and behavioral results presented here indicate that SZ patients are differentially impaired in the sensory and attentional processing of stimulus inputs that are biased toward the magnocellular versus the parvocellular visual pathway. These deficits in selecting low SF information, however, were only observed within occipital sensory processing regions. fMRI activations within parietal and frontal areas, which are hypothesized to exercise top-down control of feature-guided attention, (Corbetta 1998; Corbetta et al. 2002; Liu et al. 2003), did not differ significantly between patients and controls during attention to high and low SFs. Thus, rather than suggesting impairments in the allocation/control of attention (Fuller et al. 2006; Gold et al. 2007), the present findings support the hypothesis that the observed deficits in selective processing of attended low SF stimuli are a consequence of magnocellular-biased inputs being degraded at early stages of sensory analysis (Butler et al. 2007; Martinez et al. 2008; Javitt 2009; Kantrowitz et al. 2009).

In conclusion, although most studies of cognition in schizophrenia focus on higher order cognitive impairments such as working memory or executive processing, there is increasing appreciation of the contribution of early sensory dysfunction to these deficits (e.g., Butler et al. 2009; Sehatpour et al. 2010; Dias et al. 2011). Overall, the present study highlights the importance of considering the specific sensory properties of stimuli employed during task performance in schizophrenia, and especially their engagement of the magnocellular versus parvocellular visual pathways, in evaluating neural mechanisms underlying impaired information processing and cognitive dysfunction in SZ.

## Funding

This work was supported by grants from National Institute of Mental Health (R24MH082790, P50MH86385) and by a Young Investigator Award from the National Alliance for Research on Schizophrenia and Depression, Great Neck, NY.

## Notes

We thank Gail Silipo and Marina Shpaner for their assistance. *Conflict of Interest*: None declared.

## References

- Ammons R, Ammons C. 1962. The Quick Test (QT): provisional manual. *Psychol Rep.* 11:111–162.
- Anllo-Vento L, Hillyard SA. 1996. Selective attention to the color and direction of moving stimuli: electrophysiological correlates of hierarchical feature selection. *Percept Psychophys.* 58:191–206.
- Anllo-Vento L, Luck SJ, Hillyard SA. 1998. Spatio-temporal dynamics of attention to color: evidence from human electrophysiology. *Hum Brain Mapp.* 6:216–238.
- Arnott SR, Alain C. 2002. Effects of perceptual context on event-related brain potentials during auditory spatial attention. *Psychophysiology.* 39:625–632.
- Astafiev SV, Shulman GL, Stanley CM, Snyder AZ, Van Essen DC, Corbetta M. 2003. Functional organization of human intraparietal and frontal cortex for attending, looking, and pointing. *J Neurosci.* 23:4689–4699.
- Baas JM, Kenemans JL, Mangun GR. 2002. Selective attention to spatial frequency: an ERP and source localization analysis. *Clin Neurophysiol.* 113:1840–1854.

- Butler PD, Abeles IY, Weiskopf NG, Tambini A, Jalbrzikowski M, Legatt ME, Zemon V, Loughhead J, Gur RC, Javitt DC. 2009. Sensory contributions to impaired emotion processing in schizophrenia. *Schizophr Bull.* 35:1095–1107.
- Butler PD, Harkavy-Friedman JM, Amador XF, Gorman JM. 1996. Backward masking in schizophrenia: relationship to medication status, neuropsychological functioning, and dopamine metabolism. *Biol Psychiatry.* 40:295–298.
- Butler PD, Martinez A, Foxe JJ, Kim D, Zemon V, Silipo G, Mahoney J, Shpaner M, Jalbrzikowski M, Javitt DC. 2007. Subcortical visual dysfunction in schizophrenia drives secondary cortical impairments. *Brain.* 130:417–430.
- Butler PD, Zemon V, Schechter I, Saperstein AM, Hoptman MJ, Lim KO, Revheim N, Silipo G, Javitt DC. 2005. Early-stage visual processing and cortical amplification deficits in schizophrenia. *Arch Gen Psychiatry.* 62:495–504.
- Coleman MJ, Cestnick L, Krastoshevsky O, Krause V, Huang Z, Mendell NR, Levy DL. 2009. Schizophrenia patients show deficits in shifts of attention to different levels of global-local stimuli: evidence for magnocellular dysfunction. *Schizophr Bull.* 35:1108–1116.
- Corbetta M. 1998. Frontoparietal cortical networks for directing attention and the eye to visual locations: identical, independent, or overlapping neural systems? *Proc Natl Acad Sci U S A.* 95:831–838.
- Corbetta M, Kincade JM, Shulman GL. 2002. Neural systems for visual orienting and their relationships to spatial working memory. *J Cogn Neurosci.* 14:508–523.
- Cox RW. 1996. AFNI—software for analysis and visualization of functional magnetic resonance neuroimages. *Comput Biomed Res.* 29:162–173.
- Davis E, Graham N. 1981. Spatial frequency uncertainty effects in the detection of sinusoidal gratings. *Vision Res.* 21:705–713.
- Dias EC, Butler PD, Hoptman MJ, Javitt DC. 2011. Early sensory contributions to contextual encoding deficits in schizophrenia. *Arch Gen Psychiatry.* 68:654–664.
- Doniger GM, Foxe JJ, Murray MM, Higgins BA, Javitt DC. 2002. Impaired visual object recognition and dorsal/ventral stream interaction in schizophrenia. *Arch Gen Psychiatry.* 59:1011–1020.
- First MB, Spitzer RL, Gibbon M, Williams JBW. 1997. Structured clinical interview for DSM-IV axis I disorders—patient edition. New York: New York State Psychiatric Institute.
- Ford JM, White PM, Csernansky JG, Faustman WO, Roth WT, Pfefferbaum A. 1994. ERPs in schizophrenia: effects of antipsychotic medication. *Biol Psychiatry.* 36:153–170.
- Foxe JJ, Strugstad EC, Sehatpour P, Molholm S, Pasieka W, Schroeder CE, McCourt ME. 2008. Parvocellular and magnocellular contributions to the initial generators of the visual evoked potential: high-density electrical mapping of the “C1” component. *Brain Topogr.* 21:11–21.
- Fuller RL, Luck SJ, Braun EL, Robinson BM, McMahon RP, Gold JM. 2006. Impaired control of visual attention in schizophrenia. *J Abnorm Psychol.* 115:266–275.
- Gold JM, Fuller RL, Robinson BM, Braun EL, Luck SJ. 2007. Impaired top-down control of visual search in schizophrenia. *Schizophr Res.* 94:148–155.
- Graham N, Kramer P, Haber N. 1985. Attending to spatial frequency and spatial position of near-threshold visual patterns. In: Posner MI, Marin OSM, editors. *Attention and performance*. Hillsdale (NJ): Erlbaum. p. 269–284.
- Grave de Peralta Menendez R, Gonzalez Andino S, Lantz G, Michel CM, Landis T. 2001. Noninvasive localization of electromagnetic epileptic activity. I. Method descriptions and simulations. *Brain Topogr.* 14:131–137.
- Hansen JC, Hillyard SA. 1980. Endogenous brain potentials associated with selective auditory attention. *Electroencephalogr Clin Neurophysiol.* 49:277–290.
- Harter MR, Aine CJ. 1984. Brain mechanisms of visual selective attention. In: Parasuraman R, Davies DR, editors. *Varieties of attention*. London: Academic Press. p. 293–321.
- Heslenfeld DJ, Kenemans JL, Kok A, Molenaar PC. 1997. Feature processing and attention in the human visual system: an overview. *Biol Psychol.* 45:183–215.
- Hillyard SA, Anlo-Vento L. 1998. Event-related brain potentials in the study of visual selective attention. *Proc Natl Acad Sci U S A.* 95:781–787.
- Hopfinger JB, Buonocore MH, Mangun GR. 2000. The neural mechanisms of top-down attentional control. *Nat Neurosci.* 3:284–291.
- Javitt DC. 2009a. Sensory processing in schizophrenia: neither simple nor intact. *Schizophr Bull.* 35:1059–1064.
- Javitt DC. 2009b. When doors of perception close: bottom-up models of disrupted cognition in schizophrenia. *Annu Rev Clin Psychol.* 5:249–275.
- Kantrowitz JT, Butler PD, Schechter I, Silipo G, Javitt DC. 2009. Seeing the world dimly: the impact of early visual deficits on visual experience in schizophrenia. *Schizophr Bull.* 35:1085–1094.
- Kemali D, Galderisi S, Maj M, Mucci A, Di Gregorio M. 1991. Lateralization patterns of event-related potential and performance indices in schizophrenia: relationship to clinical state and neuroleptic treatment. *Int J Psychophysiol.* 10:225–230.
- Kiesel A, Miller J, Jolicoeur P, Brisson B. 2008. Measurement of ERP latency differences: a comparison of single-participant and jackknife-based scoring methods. *Psychophysiology.* 45:250–274.
- Kim D, Wylie G, Pasternak R, Butler PD, Javitt DC. 2006. Magnocellular contributions to impaired motion processing in schizophrenia. *Schizophr Res.* 82:1–8.
- Kurylo DD, Pasternak R, Silipo G, Javitt DC, Butler PD. 2007. Perceptual organization by proximity and similarity in schizophrenia. *Schizophr Res.* 95:205–214.
- Leitman DI, Foxe JJ, Butler PD, Saperstein A, Revheim N, Javitt DC. 2005. Sensory contributions to impaired prosodic processing in schizophrenia. *Biol Psychiatry.* 58:56–61.
- Liu T, Slotnick SD, Serences JT, Yantis S. 2003. Cortical mechanisms of feature-based attentional control. *Cereb Cortex.* 13:1334–1343.
- Livingstone MS, Hubel DH. 1987. Psychophysical evidence for separate channels for the perception of form, color, movement, and depth. *J Neurosci.* 7:3416–3468.
- Luck SJ, Gold JM. 2008. The construct of attention in schizophrenia. *Biol Psychiatry.* 64:34–39.
- Martinez A, Di Russo F, Anlo-Vento L, Hillyard SA. 2001. Electrophysiological analysis of cortical mechanisms of selective attention to high and low spatial frequencies. *Clin Neurophysiol.* 112:1980–1998.
- Martinez A, Hillyard SA, Dias EC, Hagler DJ Jr, Butler PD, Guilfoyle DN, Jalbrzikowski M, Silipo G, Javitt DC. 2008. Magnocellular pathway impairment in schizophrenia: evidence from functional magnetic resonance imaging. *J Neurosci.* 28:7492–7500.
- Michel CM, Thut G, Morand S, Khateb A, Pegna AJ, Grave de Peralta R, Gonzalez S, Seeck M, Landis T. 2001. Electric source imaging of human brain functions. *Brain Res Brain Res Rev.* 36:108–118.
- Miller J. 1981. Global precedence in attention and decision. *J Exp Psychol Hum Percept Perform.* 7:1161–1174.
- Potts GF, O'Donnell BF, Hirayasu Y, McCarley RW. 2002. Disruption of neural systems of visual attention in schizophrenia. *Arch Gen Psychiatry.* 59:418–424.
- Revheim N, Butler PD, Schechter I, Jalbrzikowski M, Silipo G, Javitt DC. 2006. Reading impairment and visual processing deficits in schizophrenia. *Schizophr Res.* 87:238–245.
- Saccuzzo DP, Braff DL. 1986. Information-processing abnormalities: trait- and state-dependent components. *Schizophr Bull.* 12:447–459.
- Schechter I, Butler PD, Zemon VM, Revheim N, Saperstein AM, Jalbrzikowski M, Pasternak R, Silipo G, Javitt DC. 2005. Impairments in generation of early-stage transient visual evoked potentials to magnocellular and parvocellular-selective stimuli in schizophrenia. *Clin Neurophysiol.* 116:2204–2215.
- Sehatpour P, Dias EC, Butler PD, Revheim N, Guilfoyle DN, Foxe JJ, Javitt DC. 2010. Impaired visual object processing across an occipital-frontal-hippocampal brain network in schizophrenia: an integrated neuroimaging study. *Arch Gen Psychiatry.* 67:772–782.
- Shulman GL, Sullivan MA, Gish K, Sakoda WJ. 1986. The role of spatial-frequency channels in the perception of local and global structure. *Perception.* 15:259–273.
- Shulman GL, Wilson J. 1987. Spatial frequency and selective attention to local and global information. *Perception.* 16:89–101.
- Slaghuis WL. 1998. Contrast sensitivity for stationary and drifting spatial frequency gratings in positive- and negative-symptom schizophrenia. *J Abnorm Psychol.* 107:49–62.

- Slaghuis WL, Bakker VJ. 1995. Forward and backward visual masking of contour by light in positive- and negative-symptom schizophrenia. *J Abnorm Psychol.* 104:41–54.
- Talairach J, Tournoux P. 1988. Co-planar stereotaxic atlas of the human brain: 3-dimensional proportional system: an approach to cerebral imaging. New York: Thieme.
- Tootell RB, Silverman MS, Hamilton SL, Switkes E, De Valois RL. 1988. Functional anatomy of macaque striate cortex. V. Spatial frequency. *J Neurosci.* 8:1610–1624.
- Wang H, Fan J. 2007. Human attentional networks: a connectionist model. *J Cogn Neurosci.* 19:1678–1689.
- Watson AB, Robson JG. 1981. Discrimination at threshold: labelled detectors in human vision. *Vision Res.* 21:1115–1122.
- Wood SM, Potts GF, Martin LE, Kothmann D, Hall JF, Ulanday JB. 2007. Disruption of auditory and visual attention in schizophrenia. *Psychiatry Res.* 156:105–116.
- Zani A, Proverbio AM. 1995. ERP signs of early selective attention effects to check size. *Electroencephalogr Clin Neurophysiol.* 95:277–292.